Journal of Advanced Scientific Research

Available online through https://sciensage.info

ISSN

0976-9595

Research Article

TiO_2-SiO_2 Nanoparticles with UV-shielding Effect and Reduced Photocatalytic Activity

Bharati Debi Biswas*

Department of Physics, Sreegopal Banerjee College, Mogra, Hooghly, West Bengal, India.

*Corresponding author: sujatab88@gmail.com

Received: 19-08-2025; Accepted: 05-09-2025; Published: 30-09-2025

https://doi.org/10.55218/JASR.2025160901

ABSTRACT

Here, we present the synthesis of multifunctional nanoparticles with suppressed photocatalytic activity, tremendous photoluminescence, great optical transparency and outstanding UV absorbance. The nanoparticles' shape is shown by FESEM tests as fibrous linkages that resemble rods and have pores in between. According to the BJH analysis, the measured pore size was 20 nm. Ultraviolet light irradiation tests confirm the highly effective UV screening performance; nevertheless, the nanoparticles' photocatalytic property was removed. In the whole 200 to 400 nm range, the UV transmittance is comparatively low, demonstrating the sample's improved UV protection capability. The nanoparticles' ultralow dimension, 2.49 m^2 g^{-1} was discovered during a nitrogen adsorption/desorption test, which is in line with their phenomenally low photocatalytic capacity.

Keywords: Nanoparticles; UV-shielding; Photoluminescence; Photocatalysis.

INTRODUCTION

Human activity has been altering the atmosphere's structure since the middle of the 1970s, which lowers the quantity of ozone found in the stratosphere.[1] Thus, it is now crucial to preserve a constant level of ozone throughout the stratosphere because, if not, UV radiation is going to eventually be accessible to diffuse to the Earth's surface with potentially catastrophic effects on all living things. Both conventional and organic UV-blocking substances are being investigated to protect against UV-Vis exposure in order to do this.[2,3] The potential of the substance to absorb ultraviolet photons, decrease the coexistence of electrons and holes generated by photosynthesis, and ultimately prevent unanticipated photocatalysis are all critical factors in the success of the UV-Vis sheltering technique.[4,5] as well as its ability to suppress the separation of photogenerated electrons and holes and eventually avoid unexpected photocatalysis.[6,7] Nanomaterials such as ZnO, CeO_2, and TiO_2 have been utilized for UV-vis shielding and to boost their UV-Vis collecting ability.[8-10] Nevertheless, there aren't many reports of successful one-pot corrosion and synchronized UV absorption synthesis. Furthermore, it continues to remain very difficult to create a UV absorption with good optical transparency because of these substance candidates' excessive refractive index and asymmetrical crystallization characteristics.[11]

Because of its exceptional photoactivity and UV filtering capabilities, TiO_2, a cheap and extremely durable semiconductor oxide, continues to be the subject of the most research out of all the inorganic compounds.[12] The nanoparticles of titanium dioxide capture ultraviolet radiation and catalyze the production of radicals containing hydroxyl and superoxide on their outermost surfaces, which can subsequently degrade organic materials. Despite the photocatalytic capability of TiO_2 must be eliminated in order to be used as UV protective coatings.[13,14] To this end, we present in our investigation the manufacturing of TiO_2-SiO_2 nanoparticles using sonochemistry, which might disrupt the production of free radicals generated by the chemical reaction of O_2 as well as H_2O alongside the electron-hole group, and tetraethyl orthosilicate (TEOS) silane as a coupling ingredient.[15] These recently created nanoparticles successfully reduce the capacity for photocatalytic degradation, ingredients and techniques.

MATERIAL AND METHODS

Synthesis of Materials

Titanium oxide (99.9%), tetraethyl orthosilicate (TEOS), and ethanol had been purchased compared to Sigma Aldrich, while sodium hydroxide pellets (NaOH) and Malachite Green oxalate dye (MG) were acquired from Merck & utilized as supplied conventionally without additional purification.

Preparation of the specimen

In order to produce a well-dispersed emulsion of TiO_2, 25 mL of ethanol was mixed in in addition to the TiO_2 NPs, and the mixture was ultrasonically sterilized for 30 minutes. Drop by drop, 1-mL containing TEOS dispersed in 1-mL of 2M NaOH was incorporated into this mixture while being vigorously stirred by a magnetic stirrer at 500 rev/sec throughout 24 hours at ambient temperature, i.e., 35°C. After filtering, the TEOS-modified TiO_2 was repeatedly cleaned with ethanol & deionized water on multiple occasions

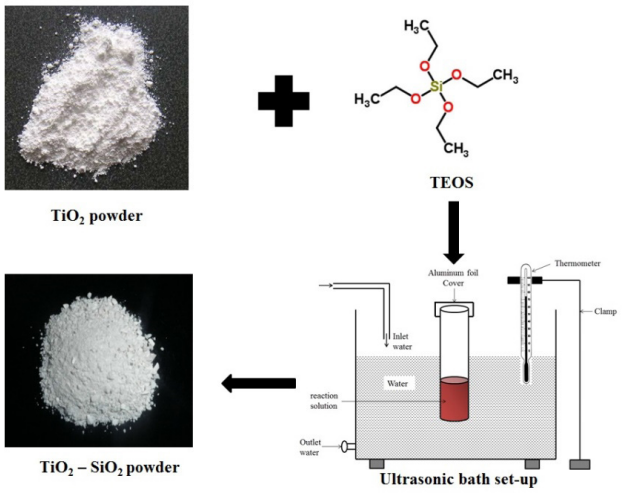

Figure 1: Synthesis of TiO_2-SiO_2 nanoparticles

before being exposed to air for 16 hours at 120°C. The TiO_2-SiO_2 nanoparticle formation method is depicted in Figure 1. Additionally, plane SiO_2 was produced while maintaining identical procedures along with additional characteristics. At the ambient temperature, tetraethyl orthosilicate and sodium hydroxide pellets were stirred thoroughly with a magnetic stirrer set at 500 rev/sec for 24 hours. After filtering, the resulting solution was repeatedly cleaned with ethanol and deionized water before being dried for 16 hours at 120°C.

Analysis of the sample

CuKα radiation wavelength λ= 0.15418 nm was used to analyze the as-synthesized compounds using XRD at a voltage gradient. In the $2\theta = 20°–80°$ range, information was gathered at a level of 0.02°. Through the use of a UV-Vis spectrophotometer, the spectrum of absorption that covers the 200–800 nm range has been determined. The photoluminescence is release by appropriate stimulation wavelength. EDS was used in conjunction with a field emission scanning electron micrograph (FESEM) type JEOL JSM-7600F to determine the specimen's morphology & elemental content. The cylindrical porosity model was used to calculate the overall distributions of pore sizes determined by the nitrogen desorption equilibrium. About 250 mL glass photo reactors were used to assess the degradation of photocatalytic enzymes using 1-mg/mL of malachite green oxalate (MG) pigment & 5 mg/mL for every photocatalyst. Four ultraviolet lamps that produced a light wave with a wavelength of 253.7 nm, a fluid circulation system (i.e., water), and a magnetic stirrer made comprised the UV irradiation arrangement (Figure 2). The entire setup was housed in a wooden enclosure that provided good insulation against the environment. In order to guarantee an adsorption-desorption state of equilibrium, photocatalytic breakdown kinetic investigations were conducted in the dark using a variety of materials exposed to UV radiation for 15 minutes using ultrasonic waves, followed by 60 minutes of stirring. The reactor was then exposed to ultraviolet light. About 2 mL of water each was collected at prearranged intervals and centrifuged right away for ten minutes at 8000 rpm. After filtering, the supernatant was examined.

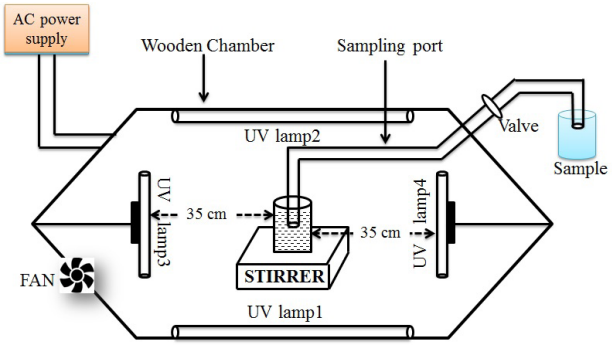

Figure 2: UV irradiation setup diagram

RESULTS AND DISCUSSIONS

Spectroscopic Characterization results

XRD analysis.

Phase is a crucial factor that affects a material's physical characteristics. Substantial diffraction peak values in the XRD structure of pure titania, as seen in Figure 3a, indicated the anatase phase (JCPDS 21-1272). Only significant anatase (JCPDS 21-1272) peaks appeared visible in the diffraction structure of TEOS-enhanced TiO_2, as shown in Figure 3b. Although SiO_2 is amorphous, no peaks were seen with Scherrer's equation [16].

$$D = K\lambda/\beta\cos\theta$$

One may determine the size of the grains (D) from peak broadening. In this equation, K is a fixed number that depends on the peak at (1.1). λ = spectrum of X-rays, β = maximum width at half maxima (FWHM) and Bragg's angle= θ

The intensity of the diffraction peaks reduced due to the margin of TiO_2 with Silica nanoparticles. The particle sizes were estimated as 20 nm. The diffraction peak intensity of the nanomaterial shows high crystallinity.

Figure 3c shows the structure of Nano SiO_2 instead of any alterations. The amorphous nature of the sample is shown by the broad, moderately intense peak that appears about 2θ~ 23°.

FESEM &EDS.

FESEM images (Figure 4a) show irregular shapes arranged in the form of rods with large voids in between. EDS images (Figure 4b) show the core elements Ti, Si and Oxygen in the composite. Extra peaks of Pt, which are shown in the figure, may be from the synthesized NaOH.

UV-visible absorption spectra

These spectra are an important tool for the comparison of the absorption of synthesized TiO_2-SiO_2 with pure TiO_2 materials. The TiO_2(titania) taken in this study for comparative purposes shows absorption maxima at 200 nm (Figure 5a) is due to non-octahedral TiO_2 species [17].SiO_2 (Figure 5b_5c) and synthesized TiO_2-SiO_2 nanoparticles both exhibit broad absorption bands spanning the visible 400–800 nm range, with absorption maxima at 200 nm. Titanium atoms are isolated on the tetrahedral silica network [18] are typically associated with this characteristic. As seen in the produced TiO_2-

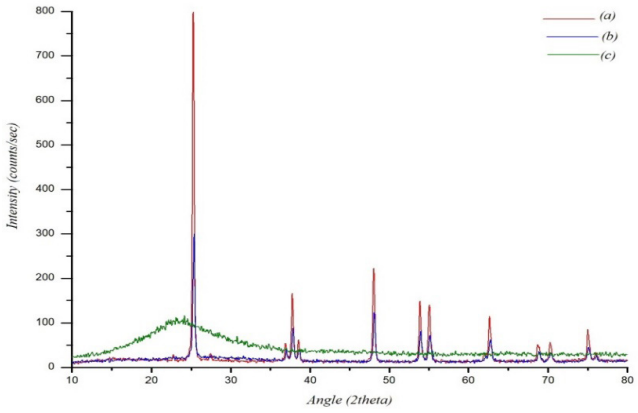

Figure 3: XRD for (a) TiO_2 anatase, (b) TiO_2-SiO_2 nanocomposites (c)SiO_2.

SiO_2 materials, the amorphous nature of the SiO_2 is accompanied by a very small particle size. However, as soon as TiO_2 is loaded, the particle size rises, and the absorption band shifts to higher wavelengths. Higher titania loading is therefore responsible for the broad absorption band in the visible spectrum that the nanoparticles display. Another indication of this reality is the XRD pattern's lack of silica peaks. Similar findings with a blue shift associated with threshold wavelength when the titania concentration drops have also been observed by Imamura et al [19].

Band gap calculation

Using the Tauc equation [20]

$$(\alpha h\nu)^n = A\ (h\nu - E_g)$$

Where hv is the amount of photon energy, A is a constant in relation to the material, α is the index of absorption, Eg is the band gap, and n is an amount that depends on the direction of changing circumstances. The band gap of the particles was determined from UV-vis absorption data. To shift the absorbing effect of radiation toward shorter wavelengths in the UV-C band, a band gap of 5.45 eV was calculated for titaniapure (inset Figure 5). While the frequency gap decreased to 4.63 eV for the created TiO_2-SiO_2 nanoparticles, it was 5.73 eV for the produced SiO_2. Because of the increased proximity of the pairs of electrons and holes and the inability to ignore the Coulombic connection that exists between both of them, large energy levels suggest confinement of the particles.[21] The reactivity of the electromagnetic spectrum to the ultraviolet UVC area is reflected in these elevated band gap energy levels.

Uv-Vis transmittance spectra

The visibility of each specimen was assessed using visual transmission tests across the UV-visible spectral range (200–800 nm). Similarly, TiO_2 and SiO_2 exhibit an ultraviolet transmission of roughly 70% at 200 nm (Figure 6a and 6c), which rises to 90% between 200 and 225 nm and stays that way throughout the visible wavelength spectrum. As a result, both TiO_2 and SiO_2 exhibit outstanding clarity across the visible spectrum, but they have inadequate UV shielding in the ultraviolet portion of the electromagnetic spectrum. TiO_2 and SiO_2particlesreflected and scattered capabilities against UV radiations might be diminished due to a certain level of nanoparticle accumulation, which could be the cause of a reduction in UV shielding.[22-23] In the situation of TiO_2 -SiO_2 nanoparticles (Figure 6b), the sample's improved ultraviolet (UV) defense property is demonstrated by the comparatively low (20%) UV transmission throughout the whole 200- 400 nm portion that comprises the electromagnetic spectrum. The produced nanoparticles exhibit improved optical quality, which suggests that they could be used as a reliable UV absorber.v

PL Energy-intensity spectra

Valence (VB) & conduction (CB), both of the bands of semiconductors, maintain their significance in amorphous states because the order of short-range determines the fundamental characteristic of electronic processes.[24] 3.69 eV was identified as a strong emission frequency band within the TiO_2 PL Wavelength-Intensity spectra (inset Figure 7a). This peak, which was seen at ambient temperature, is explained by vertical recombination. Despite its weakness, it directly demonstrates the vertical transitions of photoinduced electrons and holes in TiO_2[25]. Energy bands at 2.52, 2.68, and 2.78 eV are visible

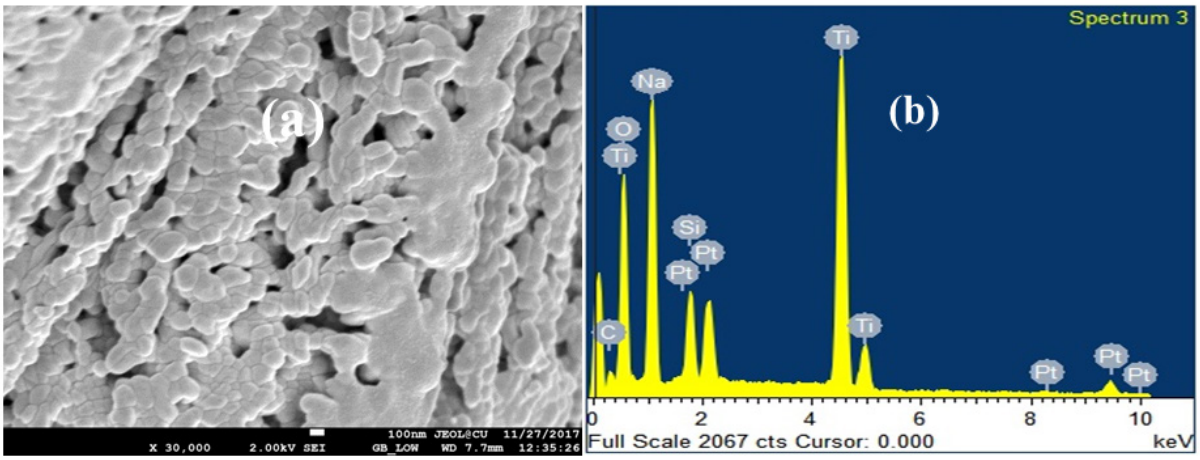

Figure 4: (a) FESEM image and (b) EDS of TiO_2-SiO_2nanoparticles

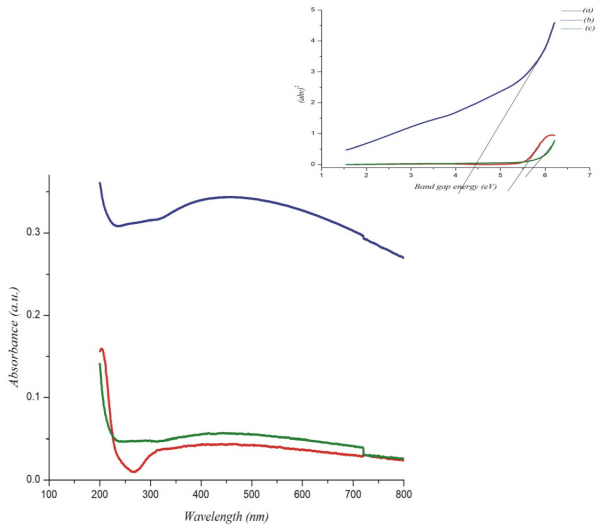

Figure 5: UV spectra (inset Tauc plot) for (a) TiO_2 anatase, (b) TiO_2-SiO_2 nanoparticles(c) SiO_2.

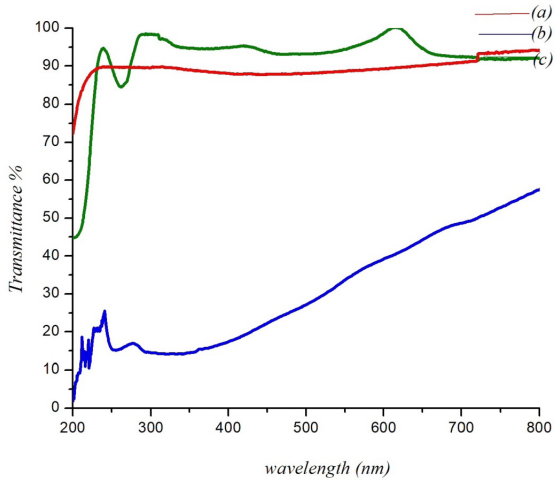

Figure6: Transmittance for(a) TiO_2 anatase, (b) TiO_2-SiO_2 nanoparticles (c) SiO_2.

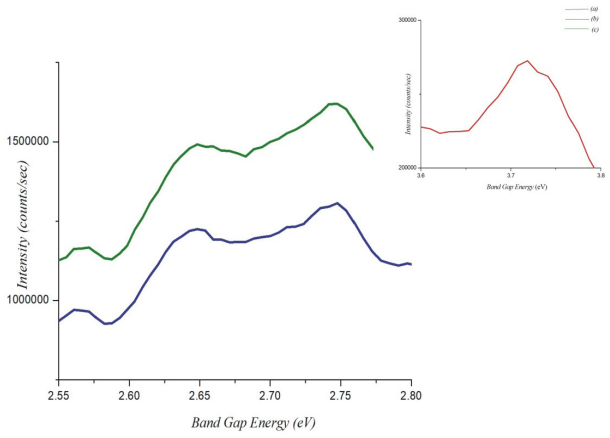

Figure 7: PL Energy- Intensity inset (a) TiO_2 anatase (b) TiO_2-SiO_2nanoparticles (c) SiO_2

in the PL Energy-Intensity bands of SiO_2 and TiO_2-SiO_2 nanoparticles (Figure 7c and 7b), respectively. The violet luminous band at 2.78 eV is due to an oxygen defect.[26,27] Experimental studies of the transient volume shift and optically detectable magnetic resonance provide evidence for the presence of the self-trapped excitation in crystalline SiO_2[24]. It is possible to attribute the unique blue fluorescence at 2.68 eV to self-trapped excitons. The emission spectra of crystalline SiO_2 also exhibit an identical luminescence band, albeit at significantly higher intensities [28]. They can then capture the excited electrons to create a singly ionization oxygen vacuum. Accordingly, self-trapped exciton particles, as suggested by [29,26], can likewise be responsible for the green luminescence spectrum at 2.52 eV. As a result, it is noted both the SiO_2 and TiO_2-SiO_2 nanoparticles exhibit strong violet & blue-green PL, suggesting potential optoelectronic uses.

BET analysis results

Brunauer- Emmett- Teller was measured porosity and surface area of TiO_2-SiO_2nanocomposites by nitrogen adsorption-desorption as shown in Figure 9[30-31]. For porous materials, adsorption and desorption branches of an isotherm curve form a loop known as a hysteresis loop seen for SBA-15 silicas [32-33].

The mesoporous characteristics observed by the Barrett-Joyner-Halenda desorption isotherm plot of pore size distributions (PSD) (Figure 9 inset). The average diameter for TiO_2-SiO_2nanooparticles is calculated by 22 nm [34]. Kruk et.al observed slightly low average diameter for SBA-15 silicas [35]. Using BET analysis surface area of synthesized nanoparticles is calculated that be 2.49 m^2g^{-1}. FESEM imaging provides evidence of the existence of large gaps in walls between adjacent pores [36]. They also reveal fibrous interconnections between the mesopores [36].

Photocatalytic degradation results

According to findings in research, TiO_2 anatase has a strong photocatalytic activity. This activity has been assigned to its increased

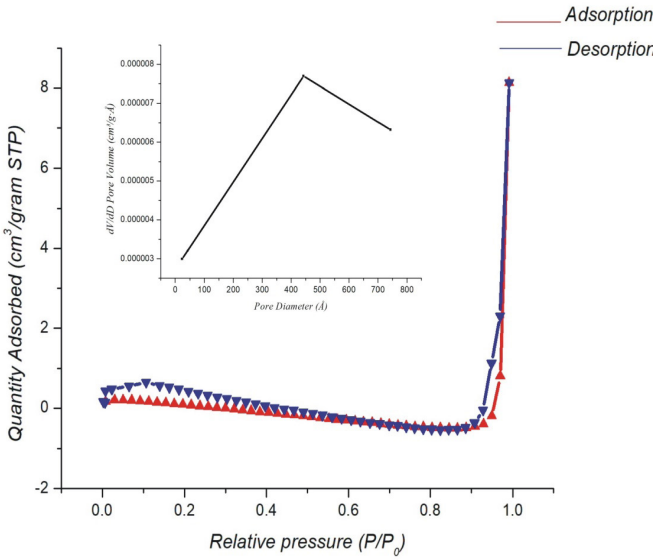

Figure 8: Nitrogen adsorption isotherms for TiO_2-SiO_2nanoparticles synthesized at 35°C (inset) pore size distribution.

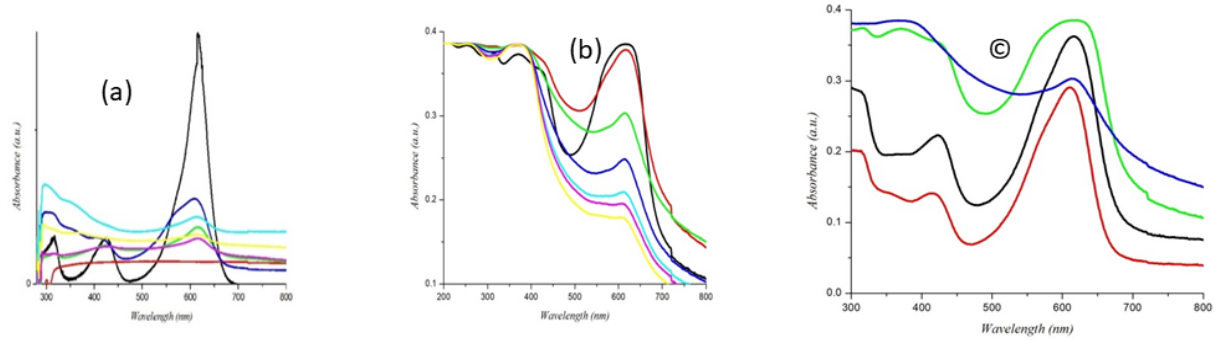

Figure 9: The photocatalysts (a) TiO_2 anatase, (b) SiO_2, and (c) TiO_2-SiO_2 nanoparticles' breakdown absorbance against wavelength figure

photo-adsorption of O_2, reduced charge recombination amount, and elevated adsorption capacities for both water molecules and hydroxyl anions [37-38]. By analyzing the velocity at which molecules broke down, synthesized photocatalytic capabilities of the TiO_2-SiO_2 nanoparticles were assessed. Using (1)[39], the chemical dyes' photocatalytic degradation activity was computed.

$$PD = \frac{(A_0 - A_t)}{A_0} \times 100, \qquad (1)$$

where A_0& A_t stand represent the dye solution's absorbance ahead of photoirradiation & the suspension solutions' wavelength following photoirradiation during t time, accordingly.

It is shown that in 180 minutes MG was degraded90.89% presence of TiO2 nanoparticles UV as shown in Figure 10a. In contrast, 5 mg/mL of SiO_2 caused 53.9% of MG (1-mg/mL) to degrade in 360 minutes (Figure 10b). In sharp contrast, the low photocatalytic activity of the produced TiO_2-SiO_2 nanoparticles only showed a 5.9, 21.2, and 25.1% decrease in MG after 1, 3, and 5 hours, respectively (Figure 10c). After this, no additional deterioration was noticed. The following is explained by the SiO_2 layer encircling the TiO_2 particles. This layer might offer a surface energy boundary that stops photoinduced holes (h+) and electrons (e-) from TiO_2 from diffusing outward.

In order to assess the potential adsorption of MG by TiO_2-SiO_2 nanoparticles, we also conducted control experiments. In the absence of ultraviolet radiation, we found that no MG was absorbed by the nanoparticles.

The photocatalytic degradation reactions are now determined by a first-order kinetic model [40]: in which the rate constant is k_1 (min^{-1}) and the MG quantities at point zero and time t (min) are denoted by C_0 & C_t (mg/L), respectively.

$$\ln\left(\frac{C_0}{C_t}\right) = k_1 t, \qquad (2)$$

Figure 11: evaluates the photocatalytic degradation of MG by each sample and correlates the k1 levels, regarding the TiO_2-SiO_2 nanoparticles be 0.00175 min-1.

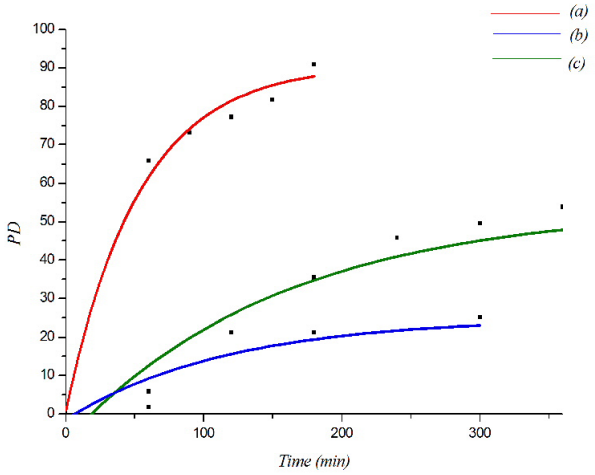

Figure 10: The degradation dynamics (PD) of the following photocatalysts (a) TiO_2 anatase, (b) TiO_2-SiO_2 nanoparticles, and (c) SiO_2 as a function of time.

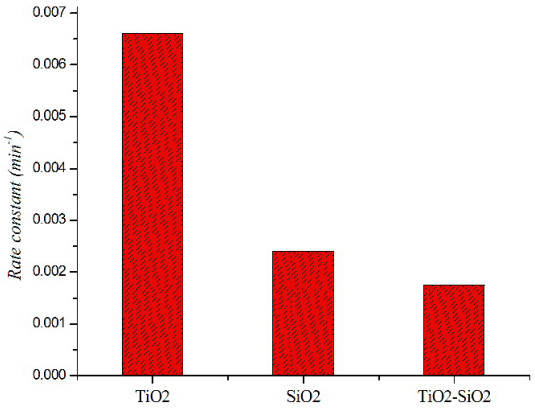

Figure 11: Rate constant bar diagram of TiO_2 anatase, TiO_2-SiO_2 nanocomposites and SiO_2.

CONCLUSION

Sol-gel synthesis of TiO_2-SiO_2 nanoparticles was accomplished effectively. The following are the main conclusions:

- There is a shift toward higher wavelengths in the absorption spectrum.
- The sample's improved UV protection is demonstrated by its comparatively low (20%). As a result, the produced nanomaterial exhibits improved optical quality, suggesting that it could be used as a reliable UV absorber. The optical quality, as evident from transmittance spectra, predicts its potential application as a biological shield and in preserving cultural artefacts and relics.
    - Luminescence studies also predict possible opto-electronic applications.
    - Texture analysis with the BET analyser indicates the mesoporous nature.
    - At a dosage of 5 mg/mL of the catalyst, the TiO_2-SiO_2 nanoparticles demonstrated a mere 25.1% malachite green presence of UV removal rate in 5 hours. Therefore, applying a coating of this nanomaterial on electronic equipment on board spacecraft may help shield its components from radiation risks and extend its service life.

ACKNOWLEDGMENT

The authors highly acknowledge the DST-FIST (SR/FST/PSI-175/2012) project, University of Kalyani and IISER Kolkata for giving me the instrumental facility.

REFERENCES

1. Sundarrajan, S., Chandrasekaran, A. R., Ramakrishna, S. 2010. An update on nanomaterials-based textiles for protection and decontamination. Journal of the American Ceramic Society., 93(12):3955–3975. https://doi.org/10.1111/j.1551-2916.2010.04117.x.
2. Montazer, M., Pakdel, E., Moghadam, M. 2010. Nano titanium dioxide on wool keratin as UV absorber stabilized by butane tetra carboxylic acid (BTCA). A statistical prospect., Fibers Polym., 11: 967–975. http://dx.doi.org/10.1007/s12221-010-0967-y.
3. World Meteorological Organization. Christine A. Ennis, Coordinating Editor. 1998. Global Ozone Research and Monitoring Project- Report No. 44. Scientific Assessment of Ozone Depletion.
4. Lima, J. F., Martins, R. F., Neri, C. R., and Serra, O. A. 2009. ''ZnO:CeO $_2$ -based nanopowders with low catalytic activity as UV absorbers'' . Appl. Surf. Sci., 255(22): 9006–9009. https://doi.org/10.1016/j.apsusc.2009.06.071.
5. Zhao, X., Zhang, F. S. Xu, Evans, D. G., and Duan, X. 2010. From Layered hydroxides to ZnO based mixed metal oxides by Thermal Decomposition: Transformation mechanism and UV blocking property of product.Chem. Mater., 22(13), 3933–3942.**[Google Scholar] [CrossRef]**
6. Li, R. Yabe, S. Yamashita, M. Momose, S. Yoshida, S. Yin, S. and Sato, T. 2002. UV-sieldin properties of zinc oxide doped ceria fine powders derived via soft solution cemicalroutes.Mater. Chem. Phys., 75(1–3):39–44. https://doi.org/10.1016/S0254-0584(02)00027-5.
7. Zholobak, N. M., Ivanov, V. K., Shcherbakov, A. B., Shaporev, A. S., Polezhaeva, O. S., Baranchikov, A. Y., Spivak, N. Y., and Tretyakov, Y. D. 2011. UV-Shieldin property, photocatalytic property, and photocytotoxicity of ceria colloid solution. J. Photochem. Photobiol., B 102(1):32–38.
8. El-Toni, A. M., Hayasaka, S., Yin, Y. and Sato, T. 2005.Coating and photochemical properties of calcia-doped ceria with amorphous silica by seeded polymerization technique. J. Mater. Chem., 15(12):1293–1297. https://doi.org/10.1016/j.jphotobiol.2010.09.002.
9. Imanaka, N., Masui, T., Hirai, H. and Adachi,G -Ya. 2003 Amorphous cerium-titanium solid solution phosphate as a novel family of Band gap of tunable sunscreem materials. Chem. Mater., 15(12): 2289–2291. http://dx.doi.org/10.1039/D1TB02604F.
10. Wang, R. H., Xin, J. H. and Tao, X. M. 2005. UV-Blocking property of dumbbell shaped ZnOcrystallines on cotton fabric.Inorg. Chem., 44(11): 3926–3930. https://pubs.acs.org/doi/10.1021/cm034200w.
11. Esch, F. Fabris, S. Zhou, L. Montini, T. Africh, C. Fornasiero, P. Comelli, G. and Rosei, R. 2005. Electron location determines defect formation on ceria substrate. Science., 309(5735): 752–755. https://doi.org/10.1126/science.1111568
12. Fujishima, A., Zhang, X.T., Tryk D.A. 2008. TiO_2 photocatalysis and related surface phenomena. Surf. Sci. Rep., 63, 515-582. https://doi.org/10.1016/j.surfrep.2008.10.001
13. Jie Xiao, Wenqin Chen, Fangyingkai Wang, and Jianzhong Du, 2013: Macromolecules 46, 375−383**.** https://doi.org/10.1021/ma3022019.
14. Dunford, R., Salinaro, A., Cai,L.Z., Serpone, N., Horikoshi, S., Hidaka, H. 1997. Chemical oxidation and DNA damaged catalyzed by inorganic sunscreen ingredient. J. FEBS Lett.., 418: 87-90. https://doi.org/10.1016/s0014-5793(97)01356-2.
15. El-Toni, A., M. Yin S., and Sato, T. J. 2006. 'Control of silica shell thickness and microporosity of titania-silica coreshell type nanoparticles to depress the photocatalytic activity of titania', J. Colloid Interface Sci., 300, 123–130.https://doi.org/10.1016/j.jcis.2006.03.073.
16. Castro, A. L., Nunes, M. R. 2008, Preparation of TiO2/SiO2 nanocomposite with non-ionic surfactants via sol-gel process and their photocatalytic study. J.Solid State Sci., *10*: 602-606.http://dx.doi.org/10.13005/ojc/300417.
17. Gontier, S. Tuel, A. 1995. Synthesis and characterization of Ti containing mesoporous silicas. Zeolites., 15: 601.https://doi.org/10.1016/0144-2449(95)00028-5.
18. Uguina, M.A., Serrano, D.P., Ovejero, van G., Grieken, Camacho, R. 1995. Preparation of TS1 by wetness impregnation by amorphous SiO_2-TiO_2 solid influence by synthesis variable. Appl. Catal. A: Gen., 124: 391.https://doi.org/10.1039/C39940000027.
19. Imamura, S., Ishida, S., Tarumoto, H., Saito, Y., Ito, T. 1993. Effect of composition of titania -silica on its physical and chemical properties. J. Chem. Soc., Faraday Trans., 89: 757.https://doi.org/10.1039/FT9938900757.
20. J. Tauc, Optical Properties of Solids (North-Holland, Amsterdam, 1970). DOI 10.1007/978-3-642-0071 https://doi.org/10.1016/j.apsusc.2011.04.1280-1.
21. Tsunekawa, S., Fukuda, T., Kasuya, A. 2000. Origin of the Blue Shift in Ultraviolet Absorption Spectra of Nanocrystalline CeO_{2-x} Particles.J. Appl. Phys., 87 :1318–1321.https://doi.org/10.2320/matertrans1989.41.1104.
22. Jiang, X.; Tian, X. Z.; Gu, J.; Huang, D.; Yang, Y. Q. 2011. "Cotton Fabric Coated with Nano TiO_2-Acrylate Copolymer for Photocatalytic Self-cleaning by In-situ Suspension Polymerization." Appl. Surf. Sci., 257:8451−8456. https://doi.org/10.1016/j.apsusc.2011.04.128
23. Asahi, R., Morikawa, T., Ohwaki, T., Aoki, K., Taga, Y.2001. Visible-Light Photocatalysis in Nitrogen-Doped Titanium Oxides. ScienceScience., 293:269−271. https://doi.org/10.1126/science.1061051.
24. Kondo, S., Itoh, T. and Saito, T. 1998. Phys. Strongly enanced optical

absorption in quenched deposited amorpous AgI films. Rev. B., **57:** 13235. DOI: https://doi.org/10.1103/PhysRevB.57.13235

25. Saini C.P., Barman A., Banerjee D., Grynko O., Prucnal S., Gupta M., Phase D.M., Sinha A.K., Kanjilal D., Skorupa W. Kanjilal A. 2017. Impact of Self-Trapped Excitons on Blue Photoluminescence in TiO2 Nanorods on Chemically Etched Si Pyramids. J. Phys. Chem. C.,121:11448−11454. DOI: 10.1021/acs.jpcc.7b02218.
26. Paleari A., Chiodini N., Di Martino D. and Meinardi F. 2005. Radioactive decay of vacuum ultra-violet excitation of silica synthesized by molecular precausor of si- si sites an indicator of intersection relaxation of neutral oxygen. Phys. Rev. B., 71 :75101. DOI: https://doi.org/10.1103/PhysRevB.71.075101
27. Kohan A. F., Ceder, G., Morgan, D. and Van de Walle, C. G. 2000. First principal study of native point defect of ZnO.Phys. Rev.B., 61: 15019
28. Trukhin, A. N. and Plaudis, A. E. 1979. Investigation of intrinsic luminescence of SiO2.Sov. Phys.Solid State., 21: 644.DOI 10.1088/0022-3719/21/26/017.
29. Sadjadi, M.S., Zare, K., Khanahmadzadeh, S., Enhessari, M. 2008. Structural characterization of NiTiO3 Nano powder prepared by stearic acid gel. Mater. Lett., 62: 3679-3681. DOI:10.1016/j.matlet.2008.04.028
30. Sing, K. S. W., Everett, D. H., Haul, R. A. W., Moscou, L., Pierotti, R. A., Rouquerol, J., Siemieniewska, T.1985. Reporting Physisorption Data Forgas/Solid Systems with Special Reference to The Determination of Surface Area and Porosity. Pure Appl. Chem., 57: 603-619. DOI:10.1351/pac198254112201.
31. Zhao, D., Feng, J., Huo, Q., Melosh, N., Frederickson, G. H., Chmelka, B. F., Stucky, G. D. 1998. Triblock copolymer synthesis of mesoporous silica with periodic 50 to 300 angstrom pore. Science, 279: 548-552. https://doi.org/10.1126/science.279.5350.548
32. Kruk, M., Jaroniec, M., Ko, C. H., Ryoo, R. 2000. Characterization of porous structure of SBA-15. Chem. Mater., 12: 1961-1968. https://pubs.acs.org/doi/10.1021/cm000164e
33. Jaroniec, M., Kruk, M., Olivier, J. P. 1999. Standard nitrogen absorption data for characterization of nanoporous silica. Langmuir., 15: 5410-5413. https://doi.org/10.1021/LA990136E
34. Kruk, M. and Langmuir, L. C. 2007, Pore size tailoring on large pore SBA-15 silica synthesized in the presence of hexane.,23: 7247-7254. DOI: 10.1021/la0702178
35. Fan, J., Yu, C., Wang, L., Tu, B., Zhao, D., Sakamoto, Y., Terasaki, O. 2001. Mesotunnels on the silica wall of the ordered SBA-15 to generate three-dimensional large pore Mesoporous network. J. Am. Chem. Soc., 123:12113-12114. https://doi.org/10.1021/ja011564l
36. Fox, M.A. and Dulay, M. 1993. Heterogenous photocatalysis Chem. Rev., 93: 341.https://pubs.acs.org/doi/10.1021/cr00017a016.
37. Ding, Z., Lu, G.Q., Greenfield, P.F. 2000. Role of crystalline phase of TiO_2 in heterogenous photocatalysis for phenol oxidation of water J. Phys. Chem. B., 104: 4585-4820. Fox, M.A. and Dulay, M. 1993. Heterogenous photocatalysis Chem. Rev., 93: 341. http://dx.doi.org/10.1021.
38. Menzinger, M Wolfgang, R.1969. The meaning and use of the Arrhenius activation energy Angew. Chem., 6: 438–444. https://doi.org/10.1002/anie.196904381
39. Al-Ekabi, H., Serpone N.1988. Kinetics Studies in Heterogeneous Photocatalysis. I. Photocatalytic Degradation of Chlorinated Phenols in Aerated Aqueous Solutions over Titania Supported on a Glass Matrix. J. Phys. Chem. 92:5726–5731. https://doi.org/10.1021/j100331a036.
40. Liu, W. Ni, J.R. Yin, X.C. 2014. Synergy of Photocatalysis and absorption for simultaneous removal of Cr (VI) and Cr (III) with TiO2 and titanate nanotubes Water Res., 53:12–25. https://doi.org/10.1016/j.watres.2013.12.043.

HOW TO CITE THIS ARTICLE: Biswas BD. TiO_2-SiO_2 Nanoparticles with UV-shielding Effect and Reduced Photocatalytic Activity. *J Adv Sci Res*. 2025;16(09): 1-7 **DOI:** 10.55218/JASR.2025160901